The Holocene
21(5) 723–734

DOI: 10.1177/0959683610386980
hol.sagepub.com
SAGE

Comparison of modeled and reconstructed changes in forest cover through the past 8000 years: Eurasian perspective

Thomas Kleinen,[1,*] Pavel Tarasov,[2,*] Victor Brovkin,[1] Andrei Andreev[3] and Martina Stebich[4]

Abstract

Reproducing the tree cover changes throughout the Holocene is a challenge for land surface–atmosphere models. Here, results of a transient Holocene simulation of the coupled climate–carbon cycle model, CLIMBER2-LPJ, driven by changes in orbital forcing, are compared with pollen data and pollen-based reconstructions for several regions of Eurasia in terms of changes in tree fraction. The decline in tree fraction in the high latitudes suggested by data and model simulations is driven by a decrease in summer temperature over the Holocene. The cooler and drier trend at the eastern side of the Eurasian continent, in Mongolia and China, also led to a decrease in tree cover in both model and data. In contrast, the Holocene trend towards a cooler climate in the continental interior (Kazakhstan) is accompanied by an increase in woody cover. There a relatively small reduction in precipitation was likely compensated by lower evapotranspiration in comparison to the monsoon-affected regions. In general the model-data comparison demonstrates that climate-driven changes during the Holocene result in a non-homogeneous pattern of tree cover change across the Eurasian continent. For the Eifel region in Germany, the model suggests a relatively moist and cool climate and dense tree cover. The Holzmaar pollen record agrees with the model for the intervals 8–3 ka and 1.7–1.3 ka BP, but suggests great reduction of the tree cover 3–2 ka and after 1.3 ka BP, when highly developed settlements and agriculture spread in the region.

Keywords

data-model comparison, Holocene, model simulations, northern and southern treeline, pollen, precipitation, summer temperature, woody cover

Introduction

The evaluation of climate model performance of simulated climates remains a challenge. While an evaluation for present-day conditions is easily possible against measurement data, no direct measurements of past climate states exist, and evaluations require the use of climate reconstructions (Wright et al., 1993).

Since the growth and composition of vegetation on a broader scale is strongly dependent on climate, pollen or plant macrofossil-derived vegetation reconstructions can provide a basis for reconstruction of past climates (Guiot, 1990; Nakagawa et al., 2002). These reconstructions can then be used to evaluate model performance (Kageyama et al., 2001; Kislov et al., 2002; Jansen et al., 2007; Wanner et al., 2008).

A second approach is to drive an equilibrium vegetation (biome) model using climate model output and to compare the simulated vegetation with the reconstructed vegetation or biome distribution (Prentice et al., 1996). This approach has, for example, been used by Harrison et al. (1998) to investigate model performance in the Palaeoclimate Modelling Intercomparison Project (PMIP) for a single point in time, a so-called time slice, 6000 years before present (6 ka BP) using the BIOME model (Prentice et al., 1992), and more recently by Wohlfahrt et al. (2008) employing the BIOME4 model (Kaplan et al., 2003) to evaluate climate model performance in the second phase of PMIP. This approach neglects feedback from the land to the atmosphere unless an iterative procedure is chosen.

In order to test whether the introduction of vegetation feedbacks produces an amplification of the response to orbital forcing at high northern latitudes sufficient to explain observed changes in regional climates, Texier et al. (1997) performed data-model comparison experiments for the Eurasian high latitudes north of 65°N and found that vegetation feedbacks indeed amplify climate changes, though changes are still underestimated.

What many previous studies have in common is that they focused on single points in time (e.g. 6 ka or 21 ka BP), as opposed to the evolution of climate and vegetation over time. With the advent of dynamic global vegetation models (DGVM) interactively coupled to climate models, it is now possible to look into the transient changes in vegetation and compare these to vegetation

[1]Max Planck Institute for Meteorology, Germany
[2]Free University of Berlin, Germany
[3]University of Cologne, Germany
[4]Senckenberg Research Institute, Research Station for Quaternary Palaeontology, Germany

Received 24 March 2010; revised manuscript accepted 12 July 2010
*These authors contributed equally to this paper.

Corresponding author:
Thomas Kleinen, Max Planck Institute for Meteorology, Bundesstr. 53, 20146 Hamburg, Germany
Email: thomas.kleinen@zmaw.de

reconstructions for multiple points in time. The use of DGVMs, fully coupled to climate models, has two major advantages: First the representation of feedbacks between vegetation and climate is much improved, and second DGVMs can also be applied in transient situations when the vegetation is not in equilibrium with climate.

Regional transient data-model comparisons have been done for some regions such as the Sahel/Sahara region (Claussen et al., 2004; Liu et al., 2007; Renssen et al., 2003), Fennoscandia (Miller et al., 2008), or the high northern latitudes (Brovkin et al., 2002), but there was no systematic study looking at different regions of Eurasia simultaneously. The present study aims to evaluate, whether the response of the coupled system of climate model and dynamic vegetation to the changes in orbital forcing over the middle and late Holocene (8 ka BP to present) is comparable with the vegetation reconstructions based on palaeobotanical data. Contrary to Gaillard et al. (2010) our aim is not to reconstruct anthropogenic changes in land cover, but rather to evaluate how the forest cover simulated by the coupled climate–vegetation model compares with pollen-derived estimates of the natural vegetation.

The biomization approach employed in some previous studies, for example the BIOME 6000 project (Prentice et al., 2000), provides no quantitative information about vegetation composition or structure (Williams et al., 2004). Quantitative information about vegetation composition and structure is of crucial importance, however, in particular for reconstructing the human impact on vegetation. This would be a prerequisite for testing the scientific hypothesis that the anthropogenic greenhouse era began about 8000 years ago as a result of intensified forest clearance and agriculture (Ruddiman, 2003; Ruddiman et al., 2008; Williams et al., 2004) (e.g. Anderson et al., 2006; Gaillard et al., 2010). In the case of a DGVM, which in our case determines plant functional types (PFT) and the evolution of their distribution over time, we decided to use a more fundamental measure than biomes. The biomization procedure already is an interpretation of the underlying data and therefore introduces additional uncertainty. We, therefore, use the model-predicted tree cover (the fraction of a grid cell covered by trees) and compare it with the published records of arboreal pollen percentages and with pollen-inferred reconstructions of woody cover. Throughout this paper we will use the terms 'tree cover' and 'woody cover' for model-predicted and pollen-inferred plant cover, respectively, because pollen-inferred reconstructions often include tall shrubs, while the model does not include a special representation of shrubs. These are represented as small trees, and therefore the expressions are used synonymously.

The current study is primarily focused on northern Asia, which was chosen because of (i) the relatively high number of sites with Holocene plant macrofossil and pollen records; (ii) the absence of late-Quaternary ice sheets and the presence of extensive areas of relatively simple topography, facilitating comparisons of proxy-based interpretations with modeling results; (iii) low population densities and relatively minor human impact on the natural vegetation; and (iv) because previous vegetation and water budget reconstructions using pollen (Rudaya et al., 2009; Tarasov et al., 2007), plant macrofossil (Kremenetski et al., 1998; MacDonald et al., 2000) and lake level records (Harrison et al., 1996) already identified northern Asia as one of the areas of the globe where significant changes in forest distribution were largely controlled by changes in temperature and atmospheric circulation patterns due to changing insolation over the Holocene. Nevertheless, the Holocene climate–vegetation interactions in northern Asia are still not as well understood as they are in other regions of the world, including the Sahara, Southeast Asia, and North America (Harrison et al., 1998; Liu et al., 2007; Prentice et al., 2000; Texier et al., 1997; Williams et al., 2004).

Data and methods

Regional setting

Northern Asia (the geographical region east of ~60°E and north of ~40°N) is at the focus of this modeling and data-model comparison study. It represents approximately 15% of the global land surface and includes a wide variety of climatic and vegetation zones. East of the Ural Mountains (~60°E) the topography is relatively flat. The elevations of West Siberia (~60–90°E) do not exceed 200 m, and elevations in Central Siberia (~90–120°E) vary around 1000 m. In the north, a band of lowlands 50–600 km wide surrounds the Arctic Ocean, while sub-longitudinal mountain ranges are typical feature of the eastern part of Siberia. Uplands and plateaus predominate in the south from Kazakhstan to Mongolia and northern China.

Northern Asia has a generally cold and continental climate. The mean January (coldest month) temperatures vary from −16°C in the south to −48°C in the inner part of Siberia and the mean July (warmest month) temperature decrease northward from 20–25°C to less than 4°C (Alpat'ev et al., 1976). Winter weather is dry and controlled by a strong Siberian anticyclone. Over two-thirds of the annual precipitation falls during the warm season, when the weather is controlled by Atlantic westerlies in the west and the southeasterly Asian summer monsoon in the southeast. Annual precipitation is highest on the western slope of the Ural Mountains (up to 600 mm) and in the easternmost areas of Russia and China, which may receive >1000 mm. Precipitation decreases to <300 mm in the inland regions of Kazakhstan, Yakutia, Mongolia and China.

The spatial distribution of vegetation reflects the latitudinal changes in insolation and longitudinal changes in precipitation, modified by altitude and slope aspect. Various types of moss, grass, and shrub tundra occupy the Arctic lowlands and the upper belt in the mountains. Southward, tundra is replaced with cold deciduous and evergreen conifer forests (taiga) dominated by larch, spruce, fir and pine species (Alpat'ev et al., 1976; Andreev and Tarasov, 2007). The northern treeline approximately follows the mean July temperature of 10–12°C (MacDonald et al., 2000). Broadleaved trees are represented mostly by cold- and drought-resistant birch and aspen species. Temperate deciduous tree taxa, such as elm, lime and oak, play a minor role in the modern vegetation. They are restricted to the wetter and warmer areas in the southern Ural, Russian Far East and northeastern China. Steppes and deserts occupy vast areas of Kazakhstan, Mongolia and northern China. Vegetation communities in transitional zones, such as forest-tundra and forest-steppe, react sensitively to changes in temperature and precipitation (Tarasov et al., 2007).

Model experiments

In this study we use results from a model experiment performed with the coupled climate–carbon cycle model CLIMBER2-LPJ. CLIMBER2-LPJ consists of the earth system model of intermediate complexity (EMIC) CLIMBER2 (Ganopolski et al., 2001; Petoukhov et al., 2000), coupled to the DGVM LPJ (Gerten et al., 2004; Sitch et al., 2003). This combination of models allows experiments on timescales of an entire interglacial because of the

low computational cost of CLIMBER2, while accounting for the heterogeneity of land surface processes on the much more highly resolved grid of LPJ.

CLIMBER2 consists of a 2.5-dimensional statistical-dynamical atmosphere with a latitudinal resolution of 10°. In the longitudinal direction the model resolves seven unevenly spaced sectors of subcontinental scale, which is equivalent to a mean longitudinal resolution of roughly 51°. It also contains an ocean model resolving three zonally averaged ocean basins with a latitudinal resolution of 2.5°, a sea ice model, and the dynamic terrestrial vegetation model VECODE (Brovkin et al., 2002). In addition, CLIMBER2 contains an oceanic biogeochemistry model, a model for marine biota (Brovkin et al., 2002, 2007; Ganopolski et al., 1998), and a weathering model.

To this EMIC we have coupled LPJ in order to investigate land surface processes at a resolution significantly higher than the resolution of CLIMBER2. LPJ is run on an 0.5°×0.5° grid and is called at the end of every model year simulated by CLIMBER2. Monthly anomalies from the climatology of the temperature, precipitation and cloudiness fields are passed to LPJ, where they are added to background climate patterns based on the Climatic Research Unit CRU-TS climate data set (New et al., 2000). In order to retain some temporal variability in these climate fields, the anomalies are not added to the climatology, but rather to the climate data for one year randomly drawn from the range 1901–1930. The change in the LPJ carbon pools is then passed back to CLIMBER2 as the carbon flux between atmosphere and land surface and is employed to determine the atmospheric CO_2 concentration for the next model year. Biogeochemical feedbacks are thus determined by the combination of CLIMBER2 and LPJ, while biogeophysical feedbacks, for example changes in albedo, are considered through the VECODE model in CLIMBER2.

Kleinen et al. (2010) performed a number of experiments with this fully coupled climate–carbon cycle model. Among these is experiment AOVPC (atmosphere–ocean–vegetation–peat–corals), which includes the carbon cycle forcing by shallow water sedimentation of calcium carbonate, as well as the accumulation of peat. This experiment reproduces the atmospheric CO_2 measured in ice cores very well and can therefore be seen as a good representation of Holocene climate–carbon cycle dynamics. In this publication we use tree cover output from that experiment and compare it with pollen-based vegetation reconstructions.

Pollen data and pollen-based woody cover reconstruction

We used a quantitative approach, which combines a vegetation cover data set derived from advanced very high resolution radiometer (AVHRR) satellite data (DeFries et al., 1999) and modern surface pollen data (Williams et al., 2004) with the best modern analogue (BMA) approach (Guiot, 1990). The approach was applied to recent and late Quaternary pollen spectra from northern Asia in order to validate the method and to reconstruct changes in woody cover (Tarasov et al., 2007). The test using modern pollen and vegetation data sets demonstrated that pollen-based reconstructions of modern woody cover and original satellite measurements match well in northern Asia. Estimates of the variance explained and the root mean square error (RMSE) for the total woody cover fraction (r^2=0.77, RMSE=11.69) are quite satisfactory at modern pollen sites (see Tarasov et al., 2007 for further details).

In order to reconstruct Holocene changes in woody cover, we applied the pollen-AVHRR-based BMA approach to a set of pollen records from northern Asia stored in the Global Pollen Database (http://www.ncdc.noaa.gov/paleo/gpd.html) and the European Pollen Database (http://www.europeanpollendatabase.net), which cover the interval between 8 ka BP and the present partly or fully. The records have non-equal temporal resolution and dating quality is not always high. The uneven spatial distribution of the pollen records is a problem for reconstruction of changes in the distribution of woody cover, since many are concentrated within a limited space, e.g. several cores are available from a single swamp or lake. In order to get insights into the major changes in regional woody cover, we first performed a reconstruction of woody cover for the 51 records which represent both time slices discussed in this paper (e.g. 8 ka and 1 ka BP). For further discussion of the regional vegetation dynamics and the background climate mechanisms, we selected several high-quality pollen records (high time resolution of the analysis and well dated sequences) representing different geographical/climatic regions within northern Asia. For each record the radiocarbon dates provided in the respective data depository were converted to calendar years before present (BP) using CalPal ver.1.4 (Danzeglocke et al., 2008). All calculations of the woody cover for the selected time slices and at the selected sites were performed using Polygon 1.5 (Nakagawa et al., 2002; http://dendro.naruto-u.ac.jp/~nakagawa/).

In order to strengthen the interpretation of the pollen-based reconstruction and model simulation results, we additionally used published data on wood macrofossils collected beyond the modern treeline in the Eurasian Arctic (Kremenetski et al., 1998; MacDonald et al., 2000) for comparison. Published pollen records from lake Holzmaar in Germany (Litt et al., 2009) and lake Sihailongwan, Northeastern China (Stebich et al., 2007), were used for comparison with model output in order to evaluate the human impact on Holocene forests. Several recently published reconstructions of atmospheric precipitation (Litt et al., 2009; Rudaya et al., 2009; Yuan et al., 2004) were also considered for comparison with the simulated climate and for the discussion of the background mechanisms of the natural forest dynamics in northern Asia through the past 8000 years.

Results and discussion

Modeled changes in climate and vegetation over the Holocene

When a model-derived map of preindustrial tree cover is compared with estimates of present-day tree cover from satellite data, a number of significant discrepancies are observed. Figure 1b shows modeled tree cover for 1 ka BP, while Figure 1c shows a satellite-derived map of present-day tree cover (DeFries et al., 1999). Overall, the model overestimates tree cover for a number of reasons. First of all, our model experiments do not contain anthropogenic forcing. Therefore modeled tree cover has to be different in all areas where anthropogenic deforestation took place, which is mainly the case in Europe and at the southern edge of the forested area, which is shown as cropland in the Loveland et al. (2000) data. In addition, the modeled northern margin of the boreal forests is located slightly further to the north, i.e. tree cover is overestimated in the high northern latitudes, though this is difficult to assess since the DeFries et al. (1999) data set has a

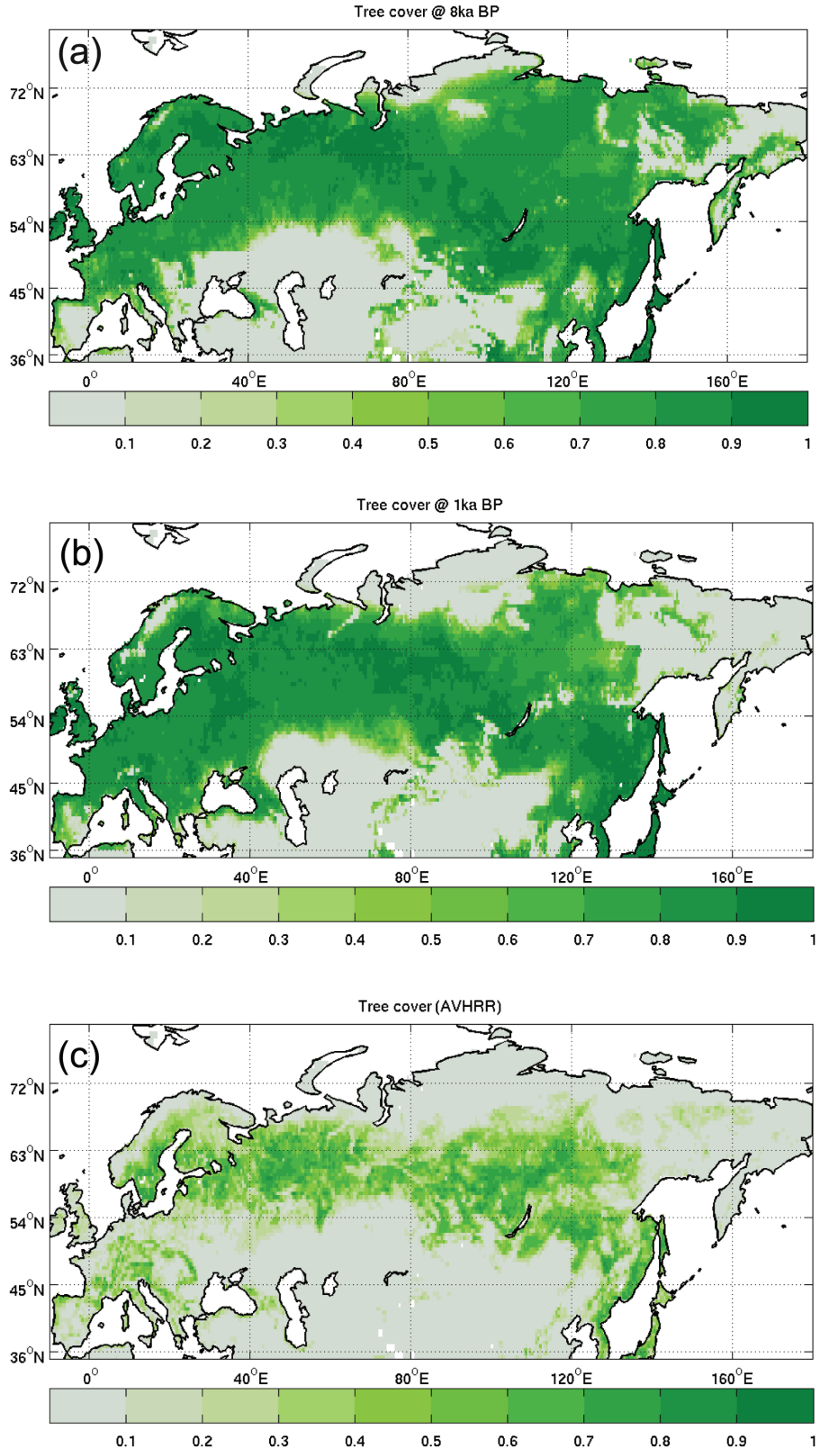

Figure 1. Eurasian model-predicted tree cover at 8 ka BP (a) and 1 ka BP (b), and tree-cover extracted from modern satellite data (c)

well-known bias in this area, while other data sets, for example Loveland et al. (2000), distinguish between forest and shrubland, where part of the shrubland would have to be counted as forest in order to be compatible with LPJ's representation of shrubs as small trees. Nevertheless, the northern tree line in LPJ also follows the July 10–12°C isotherm, in agreement with field observations (MacDonald et al., 2000). Finally the competitive advantage of trees over grasses in LPJ results in a bias towards woody plant functional types in the regions with mixed vegetation cover (Sitch et al., 2003). A comparison of absolute values of modeled tree cover with data therefore is limited in significance, and we focus on changes in tree cover instead.

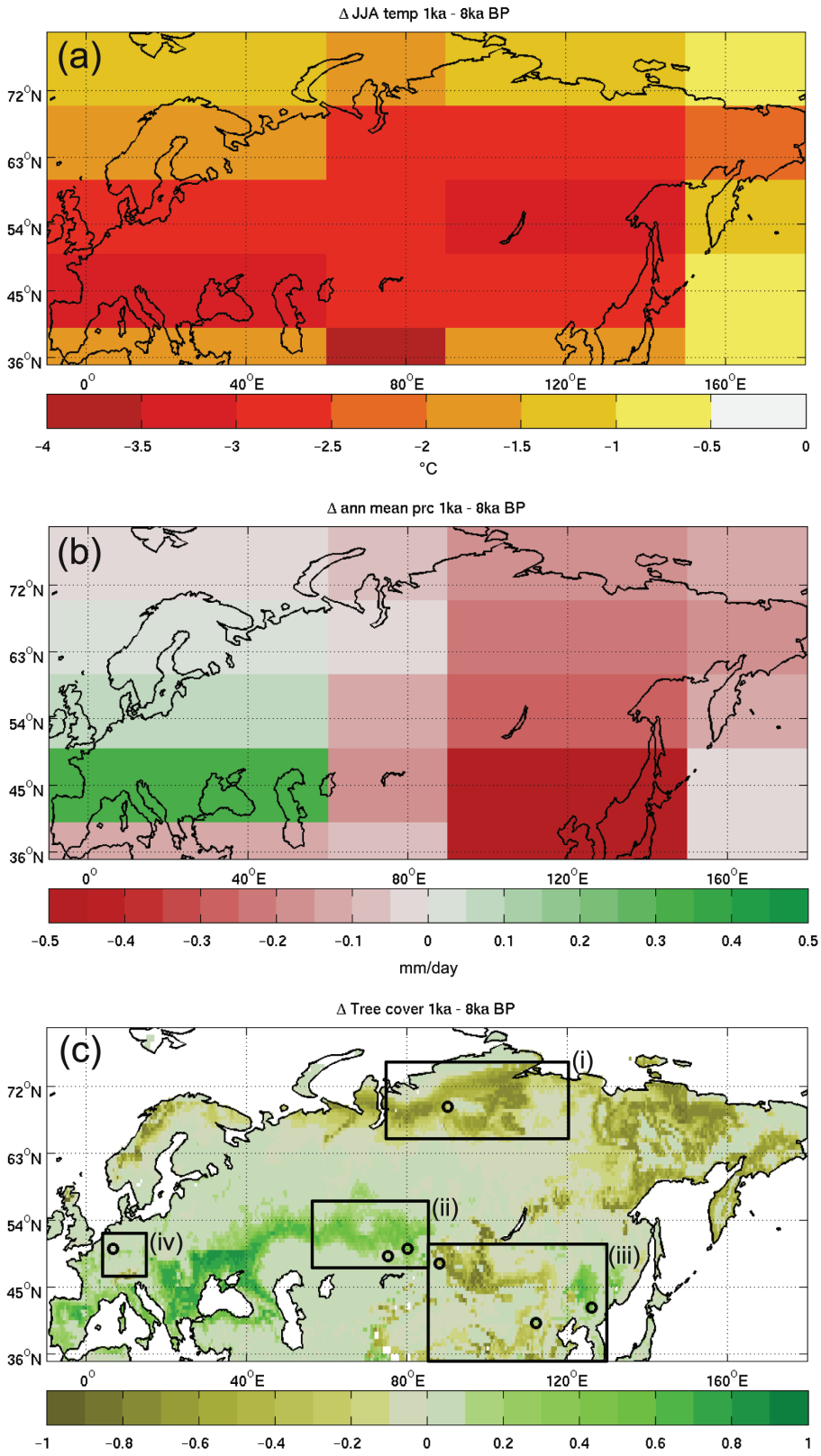

Figure 2. Model-predicted changes between 1 ka BP and 8 ka BP. (a) Summer temperature, (b) annual mean precipitation, and (c) tree cover. Circles in the map (c) indicate the locations of sites used for direct comparison of pollen-inferred woody cover and model-predicted tree cover. Boxes in (c) indicate the regions discussed in the text: (i) northern Siberia, Russia; (ii) Kazakstan; (iii) Mongolia and northern China; (iv) Germany

Over the course of the Holocene, modeled tree cover in Eurasia changes markedly. As shown in Figure 2c, the northern treeline retreats, which is especially pronounced in Siberia and Norway, while the southern forest margin moves further to the south. A decrease in tree cover is also seen in Mongolia, in an area southwest of lake Baikal.

During the time from 8 ka BP to 1 ka BP, growing-season temperatures decreased markedly all over Eurasia because of the

decrease in high latitude summer insolation. Modeled summer temperatures decreased by 2.5–3.5°C over most of Eurasia and only the northernmost parts of Scandinavia and Siberia reveal smaller amplitude changes in temperature (Figure 2a). At the same time, mean annual precipitation strongly decreased over most of Asia, particularly in the eastern part (Figure 2b). Precipitation over Europe, on the other hand, increased. Furthermore the modeling results suggest that these changes are faster and stronger before 4 ka BP, than afterwards.

With respect to the carbon cycle, the result of these changes in vegetation, as well as the increase in atmospheric CO_2 during the last 8 ka, is an increase of carbon stored on land. For Eurasia north of 40°N, total land carbon (the sum of biomass, litter, and soil carbon) increased from 743 GtC at 8 ka BP to 825 GtC at 1 ka BP, while there was a similar trend from 2020 GtC to 2120 GtC globally (Kleinen et al., 2010).

Reconstructed changes in vegetation over the Holocene

Visual comparisons of pollen-derived maps of woody cover (Figure 3a) demonstrate that the boreal forest belt in northern Asia already was fully established by 8 ka BP. The reconstruction also shows that the forest cover in the Asian mid-latitudes has changed very little between 8 ka and 1 ka BP (Figure 3b). These regions remained densely forested until modern time. This result is in line with modeling results obtained in the current study (Figure 3c, d) and corroborates with the published vegetation reconstructions based on pollen records representing different regions of Siberia. These include the Lena River valley in central Yakutia (Tarasov et al., 2007), the Ulagan plateau in southern Siberia (Blyakharchuk et al., 2004), the Lake Baikal Region (Tarasov et al., 2009) and the Amur River valley in the Russian Far East (Mokhova et al., 2009).

As in the model experiment (Figure 2), the pollen-based reconstruction (although based on a limited number of records) shows a reduction in forest cover by *c*. 5–25% between 8 ka and 1 ka BP in the high latitudes of western, central and northeastern Siberia (Figure 3). A reduction in tree cover likewise is reconstructed for the eastern part of northern Asia (e.g. Mongolia). On the other hand pollen data from Kazakhstan shows an increase in the woody cover percentage by 1 ka BP. In the following sections we present the comparison of time slice spatial patterns (Figures 2, 3) and transient series for a few selected sites representing climatically sensitive regions of northern Asia along with complementary records from Europe and China (Figures 3–6).

Arctic tundra and forest-tundra region

Lake Lama is located at the western margin of the Putorana Plateau (1701 m a.s.l.) in the southwestern part of the Taymyr Peninsula. Here, the PG1111 core (69°32′N, 90°12′E, 53 m a.s.l., see Figure 2c for region and site location), was analyzed for pollen and radiocarbon-dated (Andreev and Tarasov, 2007; Andreev et al., 2004). The area is characterized by long severe winters and a very short frost-free period. Mean July temperatures are about 10–14°C and precipitation is about 300–400 mm/yr at low elevations and up to 600–800 mm/yr on the western slopes of the Putorana Plateau (Andreev et al., 2004). Forest composed of spruce, larch and birch species grows in a narrow belt up to 200–400 m above sea level, while shrub- and herb-dominated mountain tundra occupies large areas of the region.

Figure 4a shows that modeled tree cover is slightly above 30% at 8 ka BP, which then quickly declines, reaching about 7% at 5 ka BP and declining to near zero thereafter. Reconstructed woody cover is about 20% between 8 ka BP and 4 ka BP, though fluctuating strongly, and then continues at near zero until the present day (Figure 4b). Between 8 ka and 4 ka BP, tree pollen percentages reach about 20 to 40% of the total sum, which is based on pollen and spores of terrestrial plants taken as 100%, and fluctuate around 15% after that time (Figure 4c). The total counts of radiocarbon-dated tree macrofossils stay high between 8 ka and 4 ka BP, in line with the pollen-based woody cover reconstruction, then drop to intermediate values between 4 ka and 3 ka, and stay near zero thereafter. Despite the fact that modeled tree cover declines more quickly than reconstructed woody cover, the overall magnitude of the change is rather similar. The change appears to be driven by temperature, i.e. a decrease in summer temperature of about 3°C (as shown in Figure 2a) as a result of the decrease in high latitude summer insolation.

Qualitative interpretations of pollen spectra and pollen-based biome reconstructions (e.g. Andreev and Tarasov, 2007) suggest that the predominant vegetation around lake Lama between 8 and 4 ka was boreal woodland. This is consistent with the quantitative results of the woody cover simulation and reconstruction presented here. A compilation of radiocarbon-dated tree macrofossil data from northern Eurasia (MacDonald et al., 2000) also demonstrates that boreal trees advanced to the current Arctic Ocean coast by 8 ka BP and retreated to their present position between 4.5 and 3 ka BP (Figure 4d). The northward expansion and following retreat of trees in the Arctic was attributed to the combined effect of high summer insolation (Figure 4e), low sea-ice coverage and greater continentality associated with the lower-than-present sea level (MacDonald et al., 2000; Texier et al., 1997).

Steppe and forest-steppe region

In the modern forest-steppe zone of northern Eurasia (Figures 2c, 3b, c), woody cover histories are spatially variable. Tree growth is largely controlled by moisture availability (Tarasov et al., 2007), and the area can be divided into an eastern (monsoon-controlled) and a western (westerly controlled) sector (Figures 5 and 6, respectively).

In the eastern part of our study domain, three lake sites are used for comparison (Figure 5). Hoton-Nur (48°40′N, 88°18′E, 2083 m a.s.l.) in northwestern Mongolia (Gunin et al., 1999), where alpine steppe, meadow and shrub birch tundra predominate in the regional vegetation cover. A few isolated stands of spruce and larch grow near the lake reflecting the low annual precipitation (*c*. 300 mm/yr). Two radiocarbon-dated pollen records from the lake were published (Gunin et al., 1999; Rudaya et al., 2009) and used for quantitative environmental reconstructions. Figure 5a shows about 47% simulated tree cover at 8 ka BP, with a rapid decline between 7 ka and 5 ka, when tree cover reaches about 15%. Afterwards tree cover declines slowly, until a present-day value of about 10% is reached. Reconstructed woody cover at Hoton-Nur (Figure 5b) is about 30–45% between 8 and 6 ka BP and then declines, reaching a minimum of about 5% at 3.5 ka BP. Just after 2 ka BP woody cover reaches values of 20% again, only to decline again immediately thereafter. Arboreal pollen percentages reveal a more gradual change (Figure 5c). The highest content of tree pollen (*c*. 55–65%) occurs between 8 and 6 ka BP, supporting the model outcome.

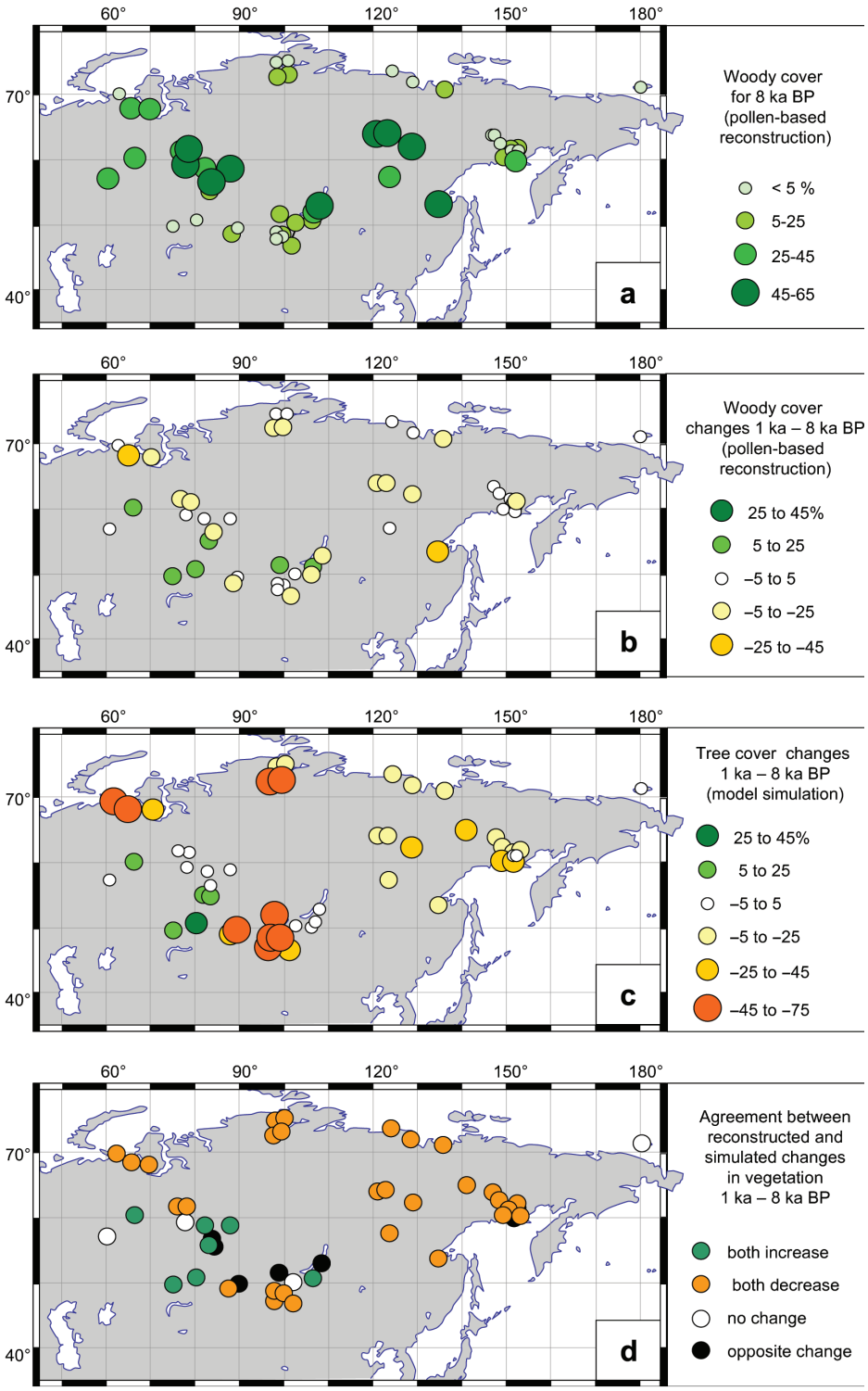

Figure 3. Charts presenting woody cover reconstruction and model simulation results at sites from northern Asia with pollen records dated to 8 ka and 1 ka BP: Reconstructed woody cover for 8 ka (a); reconstructed changes 1–8 ka (b); modelled changes 1–8 ka (c); agreement between pollen-derived and modeled changes 1–8 ka (d)

In addition there is data from two lake sites in China, lake Sihailongwan (42°17′N, 126°36′E, 791 m a.s.l.; Stebich et al., 2007) and lake Daihai (40°35′N, 112°40′E, 1220 m a.s.l.; Xiao et al., 2004). In the Sihailongwan area, which stays under strong influence of the East Asian monsoon, the precipitation averages 767 mm annually. The canopy coverage in the well-preserved forests composed of evergreen conifers and deciduous broadleaved trees is about 80–90% (Stebich et al., 2007). Simulated tree cover remains at about 90% through the past 8 ka (Figure 5d). This result is in line with more or less constant arboreal pollen percentages (Figure 5e) reaching about 90% between 8 and 4 ka BP, but oscillating around the 80% level during the past 3 ka. In the Daihai area, the situation is different. There simulated tree cover is about 80% between 8 and 3.5 ka BP and then declines slightly to about 75% (Figure 5d). The main trend is similar in the percentage curve of tree and shrub pollen, although the change is more pronounced, from about 35–45% prior to 3.5 ka BP to less than 10% at present day (Figure 5e). The area around lake Daihai was

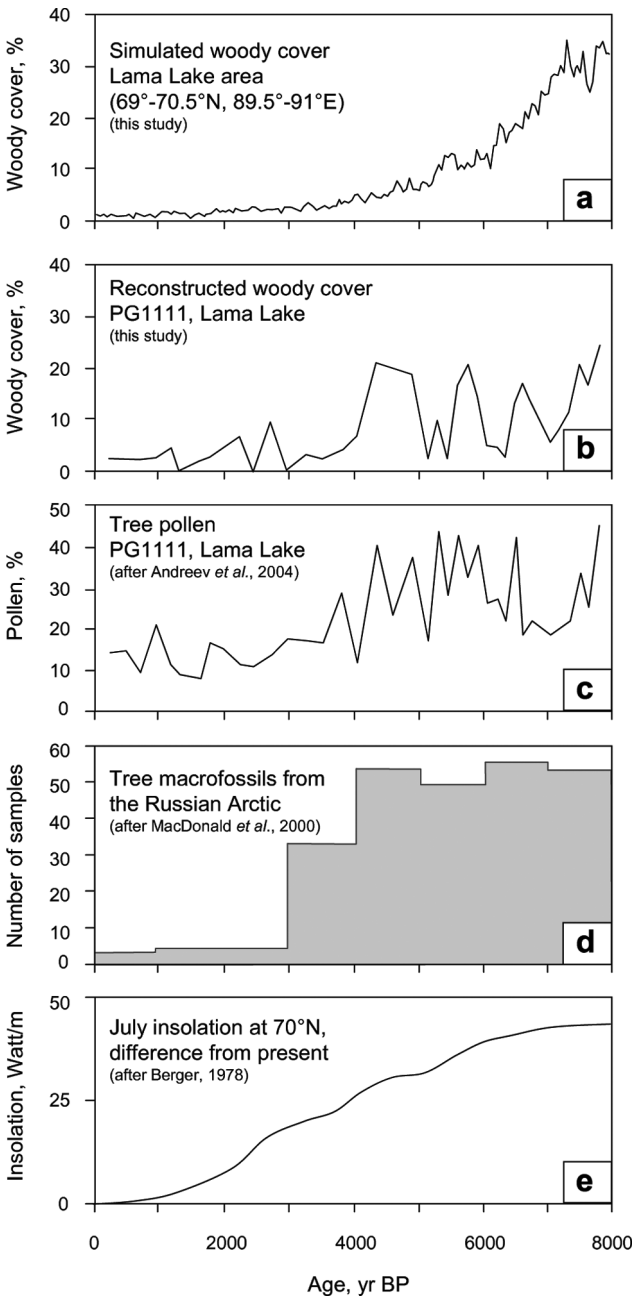

Figure 4. Charts presenting model-predicted (a) and pollen-inferred (b) changes in tree cover, and arboreal pollen percentages (c) in the Lake Lama area along with temporal distribution of radiocarbon-dated tree-macrofossils from the Eurasian Arctic north of the modern treeline (d) and summer insolation at 70°N (e) indicating a cooling trend particularly pronounced in the northern high latitudes

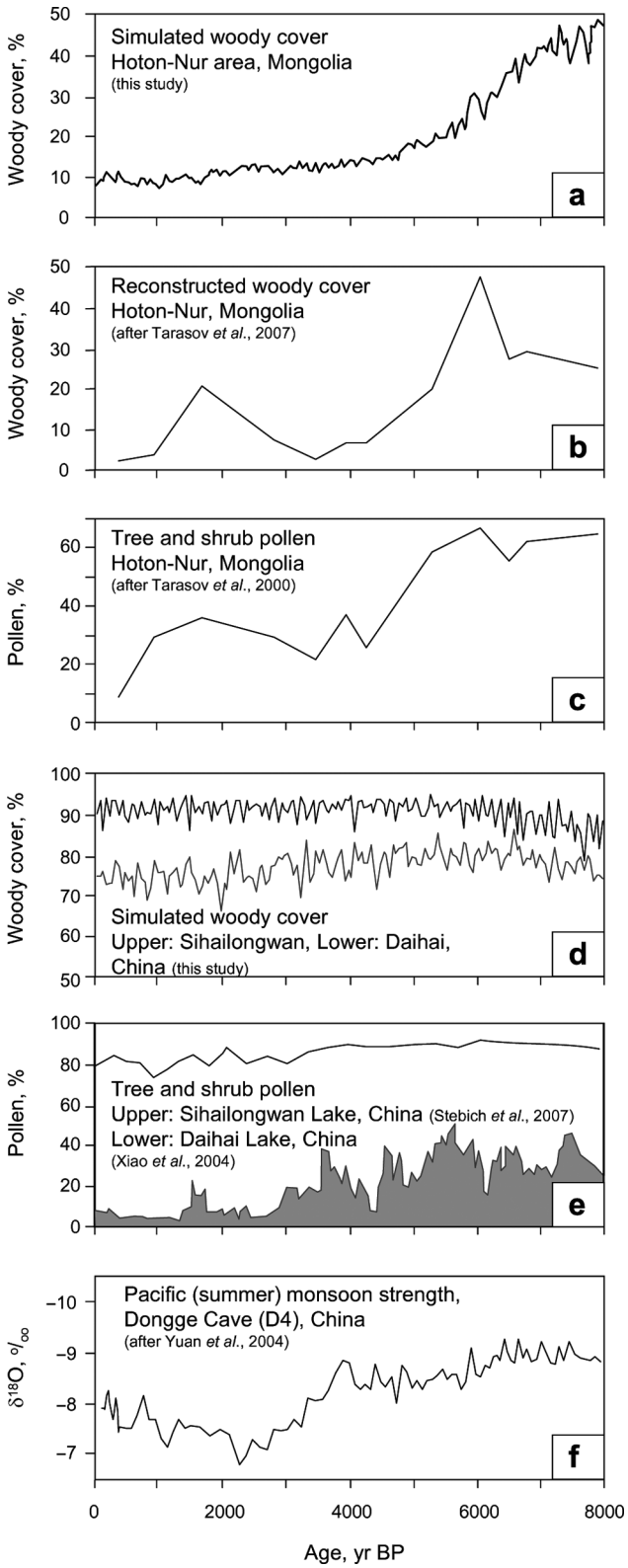

Figure 5. Charts presenting model-predicted (a, d) and pollen-inferred (b) changes in tree cover and in arboreal pollen percentages (c, e) at Hoton-Nur (a–c), Sihailongwan and Daihai (d, e) in the eastern part of mid-latitude Eurasia along with the $\delta^{18}O$ record from the Dongge Cave stalagmite (f) as proxy data for summer monsoon and atmospheric precipitation in the eastern region

intensively studied and revealed a high density of archaeological sites and continuous cultural sequence dated back to about 6.5 ka BP (Tian and Akiyama, 2001). Though human impact on the regional forest is plausible, both pollen data and model simulation suggest a decline in tree cover. Therefore, the possible impact of human activities on the regional vegetation requires more investigation.

A reconstruction of the Asian monsoon history based on the oxygen isotope record from the Dongge Cave stalagmite (Yuan et al., 2004) shows a very strong summer monsoon between 8 and 6 ka BP (Figure 5f). Weakening of the monsoon circulation since that time is reconstructed, with a phase of the weakest monsoon occurring between 3.5 and 2 ka BP. A different interpretation of the $\delta^{18}O$ changes shown by the Dongge Cave record are changes in source area, i.e. whether the area was influenced by the Indian or the Pacific monsoon (Maher, 2008). Since this would also imply a change in overall precipitation, this difference is not

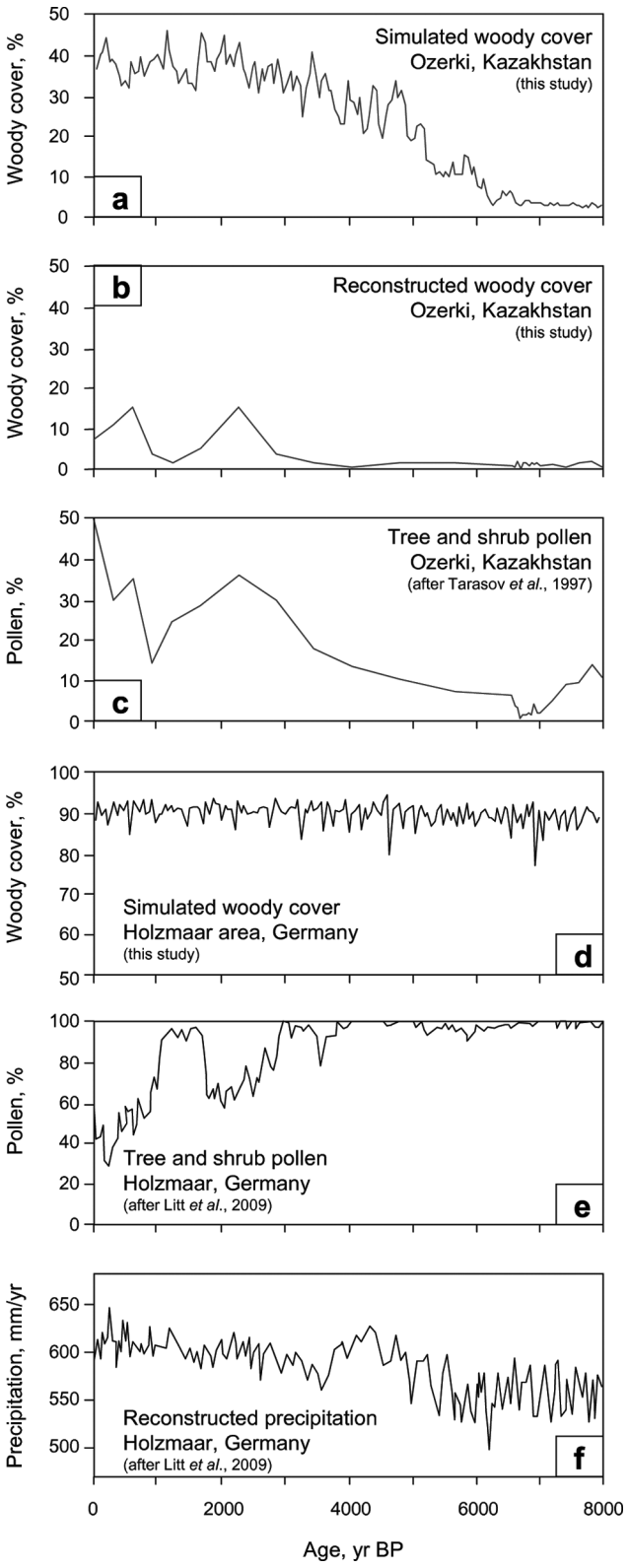

Figure 6. Charts presenting model-predicted (a, d) and pollen-inferred (b) changes in tree cover and in arboreal pollen percentages (c, e) at Ozerki (a–c) and Holzmaar (d–e) in the western part of mid-latitude Eurasia. Reconstructed annual precipitation at Holzmaar (f) indicates a general trend to progressively cooler and wetter conditions in the western region

relevant in the context of this publication. A similar change in precipitation, though more gradual than shown in Figure 5f, is also seen in the CLIMBER2 model (see Figure 2 for comparison). The decrease in tree cover in Mongolia and in north-central China, as derived from the Hoton-Nur and Daihai pollen records, is very much in line with this trend in precipitation. Annual total precipitation at the easternmost site, located close to the Pacific coast is much higher than in Mongolia. Therefore the change in precipitation is likely to have less influence on the forest vegetation there. By contrast, the precipitation reconstruction for the Hoton-Nur area demonstrates a shift from substantially wetter-than-present climate (up to 550 mm/yr) between 8 and 5 ka BP to a relatively dry climate comparable with the present after 4.5 ka BP (Rudaya et al., 2009). This reconstruction is consistent with the macrofossil-based reconstruction of taiga woods in the southern Mongolian Altai during the mid-Holocene, which would require a minimal amount of precipitation at least 100–150 mm/yr higher than present (Tarasov et al., 2000).The different amplitude of the simulated tree cover change, ranging from none close to the coast in northeastern China to very strong in northwestern Mongolia, reflects the gradient in annual total precipitation, ranging from nearly 800 mm at the coast, over 350 mm further inland to about 150 mm at the foothills of the Altai Mountains in Mongolia.

The forest development in the western sector of the northern Asian domain can be illustrated by the results from Ozerki Swamp (50°25′N, 80°28′E, 210 m a.s.l.) in Kazakhstan (Figure 6). The site is located at the upper terrace of the Irtysh River and provides the most complete radiocarbon-dated pollen record since the Lateglacial for this region (Tarasov et al., 1997). At Ozerki the simulated tree cover is near zero at 8 ka BP (Figure 6a). After 6.5 ka BP it starts increasing until it reaches about 40% just before 2 ka BP. Reconstructed woody cover also is near zero at 8 ka BP and remains at this level for longer than in the model simulation (Figure 6b). After 4 ka BP woody cover increases and reaches about 15% just before 2 ka BP. After this, woody cover remains variable, first dropping and then rising again to present-day values between 10% and 15%. The percentage of tree and shrub pollen (Figure 6c) starts rising much earlier than the reconstructed woody cover, starting at about 10% between 8 ka BP and 6 ka BP, thereafter rising to about 35% at 2.5 ka BP. Therefore reconstructed and modeled tree cover at this site behave in a similar way qualitatively, though the pollen-inferred woody cover increases much later than the model-predicted tree cover.

In contrast to the other records reviewed here, woody cover in the forest-steppe area of northern-central Kazakhstan (west of the Altai Mountains) apparently only reached modern levels during the last millennia (Tarasov et al., 2007). Further west of Ozerki, a similar trend is observed as well. In the pollen diagram from Lake Pashennoe (49°22′N, 75°24′E, 871 m a.s.l.), for example, high percentages of steppe- and desert-associated herbaceous taxa are evident throughout the early to middle Holocene (Kremenetski et al., 1997). Since 6 ka BP, pollen of birch and pine become more abundant, reflecting the gradual spread of isolated forest stands.

As at the sites in Mongolia, the reconstructed spread of boreal forests in Kazakhstan indicates increased soil moisture availability. This increase, however, is not related to changes in Pacific circulation, because regional summer and partly winter circulation and precipitation patterns currently are controlled by (1) the movement of Atlantic air masses driven by shifts in westerly flow, (2) the efficiency of hydrological recycling during the several precipitation/evaporation cycles experienced during advective water transport to the Asian interior, and (3) local to regional atmospheric processes (Tarasov et al., 2007). Various proxies from Western Europe suggest that the mid-Holocene climate (prior to

4.5 ka BP) was warm and relatively dry in comparison to the cooler and wetter late-Holocene climate (Barber et al., 2004; Snowball et al., 2004). The latter study suggested that this change was probably driven by declining summer insolation (Figure 4e) and the associated cooling of Arctic waters and reduced summer evaporation (Snowball et al., 2004). Indeed, orbitally forced PMIP simulations of the 6 ka BP climate (Braconnot et al., 2004) show higher-than-present temperature seasonality over the northern continents with summer temperatures >2°C higher-than-present in the mid-latitudinal zone between 40 and 50°N. In the eastern part of Eurasia (including China and Mongolia) this summer thermal maximum intensified land–ocean temperature contrasts and enhanced monsoonal moisture advection (Braconnot et al., 2004). However, in the western part of the continent (e.g. Kazakhstan and southwestern Siberia) situated outside of the monsoon influence, warmer-than-present summer temperatures would increase evaporation losses, thus lowering moisture availability.

Western Eurasia

In order to see whether similar trends can be observed in the westernmost part of Eurasia, where the Atlantic circulation is the chief factor controlling climate, we involved the recently published pollen record and climatic reconstruction from Lake Holzmaar (50°07′N, 6°53′E, 425 m a.s.l.) located in Germany (Litt et al., 2009) in the current discussion. At Holzmaar the model-predicted tree cover remains constant at about 90% (Figure 6d). Similar to this result, the percentage of tree and shrub pollen remains stable at about 95–99%, but shows a decline at 3 ka BP and reaches about 60% at 2 ka BP (Figure 6e). The decline then is interrupted by another millennium of tree pollen percentage near 90%, then quickly dropping again, reaching about 45% for the present day. Reconstructed precipitation, on the other hand, steadily increases over the course of the Holocene, making a climatic influence on tree cover at this site unlikely. Instead, a strong anthropogenic influence has to be acknowledged at this site (Litt et al., 2009), leading to the decrease in tree and shrub pollen due to deforestation for agriculture. The human impact was minimal during the Migration Period (between AD 300 and 700) when forests quickly regenerated and came regained equilibrium with climate, as suggested by the agreement of pollen-inferred woody cover with the model-predicted tree cover.

Conclusions

Over the last 8 ka, Eurasian climate changed markedly. High latitude summer insolation decreased, leading to a drop in summer temperature at all latitudes. At the same time, precipitation decreased over most of Eurasia, with the strongest decrease in the east Asian region controlled by the monsoon circulation, though it increased in Europe and the western sector of northern Asia, where Atlantic westerlies control modern climate.

Though CLIMBER2-LPJ generally overestimates tree cover, both for the present-day situation and for earlier times, the relative changes and main trends are consistent with the pollen-inferred quantitative and qualitative changes in woody cover. The northern treeline retreats over time, while the southern treeline expands into steppe areas in Kazakhstan and retreats in Mongolia and in the interior regions of China. Reconstructed woody cover percentages often fluctuate stronger than simulated tree cover values, particularly in the forest-steppe and forest-tundra transitional zones. This can be explained by a combination of different factors which might vary from one site to another. One of the main reasons could be generally high sensitivity of the local tree populations/individual pollen records to the short-term climate variability, which is not reproduced by the model. Changes in sedimentation, vegetation composition, fires and human activities (particularly in the southern part of the study area) may also affect the pollen spectra and therefore results of the reconstruction.

Looking at the transient changes in tree cover, one sees a generally similar development as for the pollen-inferred changes in tree cover, which is somewhat surprising, since the pollen-based estimates used in this study represent woody cover within a 21 km×21 km window around pollen sampling sites (Tarasov et al., 2007), while the model's grid-cell size is larger (0.5°x0.5°). In addition, one would expect some differences between coarse resolution results of a coupled climate–vegetation model and pollen-based reconstructions at individual sites, especially since the atmosphere model only resolves four longitudinal sectors across the study domain. In view of the approach's imperfections mentioned above, the reasonable agreement between the model-predicted tree cover and the pollen-inferred woody cover is striking, showing that many changes in vegetation can be explained by the large-scale changes in climate. Some differences in timing and amplitude of changes are apparent, though.

In the northern part of our study area, modeled tree cover retreats more quickly and more smoothly than in the reconstructions. The latter show a rather abrupt change in tree cover at about 4 ka BP, while the modeled cover changes smoothly over the first 3 ka of the time frame considered.

Similarly, in Kazakhstan in the western sector modeled tree cover starts increasing at about 6 ka BP, while the reconstruction of woody cover increases only half as strongly and not before 3 ka BP. In these parts of the study domain, the model response therefore appears to be both earlier and more gradual than the reconstructions would warrant.

The eastern part of our study domain, influenced by the summer monsoon during the early Holocene, shows a very good agreement between model and reconstruction. Both the amplitude and the timing of the changes in tree cover are very similar.

The comparison between model simulation and vegetation record/archaeological sequence from the Eifel region in Germany emphasizes the anthropogenic deforestation associated with intensive human land use and agriculture after 3 ka BP. However, modeling results match the pollen data during the archaeologically proved settlement gap in the Eifel region associated with the Migration Period.

Therefore, our modeling approach combined with vegetation records successfully evaluated the coupled climate–vegetation model. The obtained results suggest that the modeling approach used in this paper might be applied to simulate reasonable changes in past natural forest-cover and to identify periods of significant man-made deforestation or changes in forest composition in regions of the world where palaeobotanical records are rare or nonexistent, and/or intensive present land use and large modifications of the natural forest cover and composition prevent the application of the modern analogue approach.

Acknowledgements

This paper contributes to the German Research Foundation (DFG) Program 'INTERDYNAMIK' via the project 'Comparison of climate and carbon cycle dynamics during late Quaternary interglacials using a spectrum of climate system models, ice-core and terrestrial archives'

(TA 540/1-2, BR 2950/2-2). We would like to thank Anne Dallmeyer, who commented on an earlier version of this manuscript, as well as three anonymous reviewers who provided very helpful comments.

References

Alpat'ev AM, Arkhangel'skii AM, Podoplelov NY and Stepanov AY (1976) *Physical Geography of the USSR (Asiatic Part)*. Vysshaya Shkola.

Anderson J, Bugmann H, Dearing JA and Gaillard M-J (2006) Linking palaeoenvironmental data and models to understand the past and to predict the future. *Trends in Ecology and Evolution* 21(12): 696–704.

Andreev AA and Tarasov PE (2007) Pollen records, postglacial: northern Asia. In: Elias S (ed.) *Encyclopedia of Quaternary Science 4.* Elsevier, 2721–2729.

Andreev AA, Tarasov PE, Klimanov VA, Melles M, Lisitsyna OM and Hubberten HW (2004) Vegetation and climate changes around the Lama Lake, Taymyr Peninsula, Russia during the Late Pleistocene and Holocene. *Quaternary International* 122: 69–84.

Barber K, Zolitschka B, Tarasov P and Lotter AF (2004) Atlantic to Urals – The Holocene climatic record of mid-latitude Europe. In: Battarbee RW, Gasse F and Stickley CE (eds) *Past Climate Variability through Europe and Africa.* Developments in Paleoenvironmental Research 6. Springer, 417–442.

Blyakharchuk TA, Wright HE, Borodavko PS, van der Knaap WO and Ammann B (2004) Late-glacial and Holocene vegetational changes on the Ulagan high-mountain plateau, Altai Mountains, southern Siberia. *Palaeogeography, Palaeoclimatology, Palaeoecology* 209: 259–279.

Braconnot P, Harrison SP, Joussaume S, Hewitt CD, Kitoh A, Kutzbach JE et al. (2004) Evaluation of PMIP coupled ocean–atmosphere simulations of the mid-Holocene. In: Battarbee RW, Gasse F and Stickley CE (eds) *Past Climate Variability through Europe and Africa.* Developments in Paleoenvironmental Research 6. Springer, 515–550.

Brovkin V, Bendtsen J, Claussen M, Ganopolski A, Kubatzki C, Petoukhov V et al. (2002) Carbon cycle, vegetation, and climate dynamics in the Holocene: Experiments with the CLIMBER-2 model. *Global Biogeochemical Cycles* 16: 1139, doi:10.1029/2001GB001662.

Brovkin V, Ganopolski A, Archer D and Rahmstorf S (2007) Lowering of glacial atmospheric CO_2 in response to changes in oceanic circulation and marine biogeochemistry. *Paleoceanography* 22: PA4202, doi:10.1029/2006PA001380.

Claussen M, Cox PM, Zeng X, Viterbo P, Beljaars ACM, Betts R et al. (2004) The global climate. In: Kabat P, Claussen M, Dirmeyer PA, Gash JHC, Guenni L, Meybeck M et al. (eds) *Vegetation, Water, Humans and the Climate: A New Perspective on an Interactive System*. Heidelberg: Springer-Verlag, Chapter A.4, 33–57.

Danzeglocke U, Jöris O and Weninger B (2008) CalPal-2007online. http://www.calpal-online.de

DeFries RS, Townshend JRG and Hansen MC (1999) Continuous fields of vegetation characteristics at the global scale at 1km resolution. *Journal of Geophysical Research* 104: 16 911–16 925.

Gaillard M-J, Sugita S, Mazier F, Kaplan JO, Trondman A-K, Broström A et al. (2010) Holocene land-cover reconstructions for studies on land cover–climate feedbacks. *Climate of the Past* 6: 483–499.

Ganopolski A, Rahmstorf S, Petoukhov V and Claussen M (1998) Simulation of modern and glacial climates with a coupled global climate model. *Nature* 391: 351–356.

Ganopolski A, Petoukhov V, Rahmstorf S, Brovkin V, Claussen M, Eliseev A et al. (2001) CLIMBER-2: A climate system model of intermediate complexity. Part II: Model sensitivity. *Climate Dynamics* 17: 735–751.

Gerten D, Schaphoff S, Haberlandt U, Lucht W and Sitch S (2004) Terrestrial vegetation and water balance – Hydrological evaluation of a dynamic global vegetation model. *Journal of Hydrology* 286: 249–270.

Guiot J (1990) Methodology of the last climatic cycle reconstruction from pollen data. *Palaeogeography, Palaeoclimatology, Palaeoecology* 80: 49–69.

Gunin PD, Vostokova EA, Dorofeyuk NI, Tarasov PE and Black CC (1999) *Vegetation Dynamics of Mongolia*. Springer Verlag.

Harrison SP, Yu G and Tarasov PE (1996) Late Quaternary lake-level record from northern Eurasia. *Quaternary Research* 45: 138–159.

Harrison SP, Jolly D, Laarif F, Abe-Ouchi A, Dong B, Herterich K et al. (1998) Intercomparison of simulated global vegetation distributions in response to 6 kyr BP orbital forcing. *Journal of Climate* 11: 2721–2742.

Jansen E, Overpeck J, Briffa KR, Duplessy J-C, Joos F, Masson-Delmotte V et al. (2007) Palaeoclimate. In: Solomon S, Qin D, Manning M, Chen Z, Marquis M, Averyt KB et al. (eds) *Climate Change 2007: The Physical Science Basis.* Contribution of Working Group I to the Fourth Assessment Report of the Intergovernmental Panel on Climate Change. Cambridge/New York: Cambridge University Press.

Kageyama M, Peyron O, Pinot S, Tarasov P, Guiot J, Joussaume S et al. (2001) The Last Glacial Maximum climate over Europe and western Siberia: A PMIP comparison between models and data. *Climate Dynamics* 17: 23–43.

Kaplan JO, Bigelow NH, Prentice IC, Harrison SP, Bartlein PJ, Christensen TR et al. (2003) Climate change and arctic ecosystems II. Modeling, paleodata-model comparisons, and future projections. *Journal of Geophysical Research* 108: 8171, doi:10.1029/2002JD002559.

Kislov AV, Tarasov PE and Sourkova GV (2002) Pollen and other proxy-based reconstructions and PMIP simulations of the Last Glacial Maximum mean annual temperature: An attempt to harmonize the data-model comparison procedure. *Acta Palaeontologica Sinica* 41: 539–545.

Kleinen T, Brovkin V, von Bloh W, Archer D and Munhoven G (2010) Holocene carbon cycle dynamics. *Geophysical Research Letters* 37: L02705, doi:10.1029/2009GL041391.

Kremenetski CV, Sulerzhitsky LD and Hantemirov R (1998) Holocene history of the northern range limits of some trees and shrubs in Russia. *Arctic and Alpine Research* 30: 317–333.

Kremenetski V, Tarasov P and Cherkinsky E (1997) Postglacial development of Kazakhstan pine forests. *Geographie physique et Quaternaire* 51: 391–404.

Litt T, Schölzel C, Kühl N and Brauer A (2009) Vegetation and climate history in the Westeifel Volcanic Field (Germany) during the past 11 000 years based on annually laminated lacustrine maar sediments. *Boreas* 38: 679–690.

Liu Z, Wang Y, Gallimore R, Gasse F, Johnson T, deMenocal P et al. (2007) Simulating the transient evolution and abrupt change of Northern Africa atmosphere–ocean–terrestrial ecosystem in the Holocene. *Quaternary Science Reviews* 26: 1818–1837.

Loveland TR, Reed BC, Brown JF, Ohlen DO, Zhu J, Yang L et al. (2000) Development of a Global Land Cover Characteristics Database and IGBP DISCover from 1-km AVHRR Data. *International Journal of Remote Sensing* 21: 1303–1330.

MacDonald GM, Velichko AA, Kremenetski CV, Borisova OK, Goleva AA, Andreev AA et al. (2000) Holocene treeline history and climate change across Northern Eurasia. *Quaternary Research* 53: 302–311.

Maher BA (2008) Holocene variability of the East Asian summer monsoon from Chinese cave records: A re-assessment. *The Holocene* 18: 861–866.

Miller PA, Kiesecke T, Hickler T, Bradshaw RHW, Smith B, Seppä H et al. (2008) Exploring climatic and biotic controls on Holocene vegetation change in Fennoscandia. *Journal of Ecology* 96: 247–259.

Mokhova L, Tarasov P, Bazarova V and Klimin M (2009) Quantitative biome reconstruction using modern and late Quaternary pollen data from the southern part of the Russian Far East. *Quaternary Science Reviews* 28: 2913–2926.

Nakagawa T, Tarasov P, Kotoba N, Gotanda K and Yasuda Y (2002) Quantitative pollen-based climate reconstruction in Japan: Application to surface and late Quaternary spectra. *Quaternary Science Reviews* 21: 2099–2113.

New M, Hulme M and Jones P (2000) Representing twentieth-century space–time climate variability. Part II: Development of 1901–96 monthly grids of terrestrial surface climate. *Journal of Climate* 13: 2217–2238.

Petoukhov V, Ganopolski A, Brovkin V, Claussen M, Eliseev A, Kubatzki C et al. (2000) CLIMBER-2: A climate system model of intermediate complexity. Part I: Model description and performance for present climate. *Climate Dynamics* 16: 1–17.

Prentice IC, Cramer W, Harrison SP, Leemans R, Monserud RA and Solomon AM (1992) A global biome model based on plant physiology and dominance, soil properties, and climate. *Journal of Biogeography* 19: 117–134.

Prentice IC, Guiot J, Huntley B, Jolly D and Cheddadi R (1996) Reconstructing biomes from palaeoecological data: A general method and its application to European pollen data at 0 and 6 ka. *Climate Dynamics* 12: 185–194.

Prentice IC, Jolly D and BIOME 6000 Participants (2000) Mid-Holocene and glacial maximum vegetation geography of the northern continents and Africa. *Journal of Biogeography* 27: 507–519.

Renssen H, Brovkin V, Fichefet T and Goosse H (2003) Holocene climate instability during the termination of the African Humid Period. *Geophysical Research Letters* 30: 1184, doi:10.1029/2002GL016636.

Rudaya N, Tarasov P, Dorofeyuk N, Solovieva N, Kalugin I, Andreev A et al. (2009) Holocene environments and climate in the Mongolian Altai reconstructed from the Hoton-Nur pollen and diatom records: A step towards better understanding climate dynamics in Central Asia. *Quaternary Science Reviews* 28: 540–554.

Ruddiman WF (2003) The anthropogenic greenhouse era began thousands of years ago. *Climatic Change* 61: 261–293.

Ruddiman WF, Guo Z, Zhou X, Wu H and Yu Y (2008) Early rice farming and anomalous methane trends. *Quaternary Science Reviews* 27: 1291–1295.

Sitch S, Smith B, Prentice IC, Arneth A, Bondeau A, Cramer W et al. (2003) Evaluation of ecosystem dynamics, plant geography and terrestrial carbon cycling in the LPJ dynamic global vegetation model. *Global Change Biology* 9: 161–185.

Snowball I, Korhola A, Briffa KR and Koç N (2004) Holocene climate dynamics in Fennoscandia and theNorth Atlantic. In: Battarbee RW, Gasse F and Stickley CE (eds) *Past Climate Variability through Europe and Africa.* Developments in Paleoenvironmental Research 6. Springer, 364–397.

Stebich M, Arlt J, Liu Q and Mingram J (2007) Late Quaternary vegetation history of Northeast China – Recent progress in the palynological investigations of Sihailongwan maar lake. *Courier Forschungsinstitut Senckenberg* 259: 181–190.

Tarasov P, Jolly D and Kaplan J (1997) A continuous Late Glacial and Holocene record of vegetation changes in Kazakhstan. *Palaeogeography, Palaeoclimatology, Palaeoecology* 136: 281–292.

Tarasov P, Dorofeyuk N and Metel'tseva E (2000) Holocene vegetation and climate changes in Hoton-Nur basin, northwest Mongolia. *Boreas* 29, 117–126.

Tarasov P, Williams JW, Andreev A, Nakagawa T, Bezrukova E, Herzschuh U et al. (2007) Satellite- and pollen-based quantitative woody cover reconstructions for northern Asia: Verification and application to late-Quaternary pollen data. *Earth and Planetary Science Letters* 264: 284–298.

Tarasov PE, Bezrukova EV and Krivonogov SK (2009) Late glacial and Holocene changes in vegetation cover and climate in southern Siberia derived from a 15 kyr long pollen record from Lake Kotokel. *Climate of the Past* 5: 73–84.

Texier D, de Noblet N, Harrison SP, Haxeltine A, Jolly D, Joussaume S et al. (1997) Quantifying the role of biosphere–atmosphere feedbacks in climate change: Coupled model simulations for 6000 years BP and comparison with palaeodata for northern Eurasia and northern Africa. *Climate Dynamics* 13: 865–882.

Tian GJ and Akiyama S (2001) *Archaeological Excavations at Daihai (II)*. Beijing: Science Press.

Wanner H, Beer J, Bütikofer J, Crowley TJ, Cubasch U, Flückiger J et al. (2008) Mid- to Late Holocene climate change: An overview. *Quaternary Science Reviews* 27: 1791–1828.

Williams JW, Shuman BN,Webb T III, Bartlein PJ and Leduc PL (2004) Late Quaternary vegetation dynamics in North America: Scaling from taxa to biomes. *Ecological Monographs* 74: 309–334.

Wohlfahrt J, Harrison SP, Braconnot P, Hewitt CD, Kitoh A, Mikolajewicz U et al. (2008) Evaluation of coupled ocean–atmosphere simulations of the mid-Holocene using palaeovegetation data from the northern hemisphere extratropics. *Climate Dynamics* 31: 871–890.

Wright HE, Kutzbach JE, Webb T III, Ruddiman WD, Street-Perrott FA and Bartlein PJ (1993) *Global Climates Since the Last Glacial Maximum*. University of Minnesota Press.

Xiao J, Xu Q, Nakamura T, Yang X, Liang W and Inouchi Y (2004) Holocene vegetation variation in the Daihai Lake region of north-central China: A direct indication of the Asian monsoon climatic history. *Quaternary Science Reviews* 23: 1669–1679.

Yuan D, Cheng H, Edwards RL, Dyoski CA, Kelly MJ, Zhang M et al. (2004) Timing, duration, and transitions of the last interglacial Asian monsoon. *Science* 304: 575–578.